

Many-Body Polarization, a Cause of Asymmetric Solvation of Ions and Quadrupoles

Anders Öhrn* and Gunnar Karlström

*Department of Theoretical Chemistry, Chemical Center, P.O. Box 124,
S-221 00 Lund, Sweden*

Received January 22, 2007

Abstract: Three models are used to study the effect of many-body polarization in the solvation of non-dipolar molecules and ions in water. Two of the models are very simplified and are used to show a number of basic principles of correlation of solvent degrees of freedom and asymmetric solvent structures. These principles are used to interpret results from the third model: an accurate simulation of para-benzoquinone (PBQ) in aqueous solution with a combined quantum chemical statistical mechanical solvent model with an explicit solvent. It is found that nonzero polarizability of PBQ introduces correlation in the solvent degrees of freedom through the many-body nature of the polarization. The fluctuating electric field from the solvent on the solute increases in magnitude with the correlation. Solvent effects are hence modified. This correlation is not described within the mean-field approximation. In practice, the correlation will show up as an increased probability for asymmetric solvation of the molecule.

1. Introduction

The solvation of molecules in liquid solvent or large organic assemblies, such as proteins or micelles, constitutes a large and important part of chemistry. Most chemistry, after all, takes place in an environment. Along improving computers and quantum chemical methods, our comprehension and ability to predict properties of molecular matter have been taken to new levels of detail, accuracy, and size. Useful as this may be, to be able to pinpoint and characterize the features relevant to the question of the particular system and thus get a better understanding, nontrivial simplifications are needed by definition. This article is meant to attain good understanding of a molecular system in aqueous solution studied in a previous article with an accurate model.¹ We wish to establish the relevant aspect of the system for a property that was found in the results.

The system is para-benzoquinone (PBQ) surrounded by water at room temperature. For this system, it is found that the solvent structure in the vicinity of the two carbonyl groups is correlated in such a way that asymmetric structures are favored. On the basis of a qualitative comparison with studies on solvation of ions and their affinity to surfaces, it

was suggested that the many-body polarization of PBQ was the cause of this observation.^{2–6} To test and refine this statement, we will use three different models, all involving different simplifications, in order to properly investigate the problem.

The results obtained and presented below give credence to the claim that many-body polarization indeed is the relevant aspect for understanding the correlation and asymmetry that is observed. PBQ in aqueous solution is, however, not the only system for which polarization can have this influence. Rather, we argue that it can be of importance to a much wider set of solvation problems, especially in polar environments. The many-body effects that are found to be of importance are disregarded in a mean-field approximation. The molecular nature of the solvent and a more detailed statistical mechanical treatment have to be considered in order to account for these effects.

2. Models and Results

Three models are used to address the question of this article. The first two are very simple models that do not treat the problem in its full complexity. They will instead unambiguously demonstrate simple relations. These relations are then used to analyze the results of the third model, which is a

* Corresponding author e-mail: anders.ohrn@teokem.lu.se

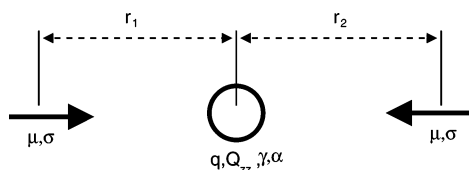


Figure 1. One-dimensional model system A. The central particle can have charge, quadrupole, and polarizability; the peripheral particles have dipoles of equal magnitude, but of opposite direction.

realistic simulation of PBQ in aqueous solution at room temperature.

2.1. Polarizable Trimer. The one-dimensional model system A is depicted in Figure 1. It consists of three particles: one central polarizable particle with either charge, q , or quadrupole, Q_{zz} , and two peripheral particles with dipoles of equal magnitude, $|\mu|$, but of opposite orientation. The potential energy of model system A is

$$U(r_1, r_2) = \left(\frac{\sigma + \gamma}{2r_1}\right)^{12} + \left(\frac{\sigma + \gamma}{2r_2}\right)^{12} + \left(\frac{\sigma}{r_1 + r_2}\right)^{12} + \frac{2|\mu|^2}{(r_1 + r_2)^3} + 3\frac{Q_{zz}|\mu|}{r_1^4} + 3\frac{Q_{zz}|\mu|}{r_2^4} + \frac{q|\mu|}{r_1^2} + \frac{q|\mu|}{r_2^2} - 2|\mu|^2\alpha\left(\frac{1}{r_1^3} - \frac{1}{r_2^3}\right)^2 \quad (1)$$

The first three terms are the Lennard-Jones repulsion between all particles; parameters σ and γ denote the sizes of the peripheral and the central particles, respectively. The fourth term is the repulsive dipole–dipole interaction between the two peripheral particles. The next four terms will all be attractive in the present application and derive from electrostatic pair interactions between peripheral and central particles. The final term is the induction energy from the polarizability, α , on the central particle. Correlation is obtained if the joint-probability function for r_1 and r_2 , $p(r_1, r_2)$, cannot be written as a product of two functions that only depends on either variable. Fundamental results of statistical mechanics give that $p(r_1, r_2) = e^{-U(r_1, r_2)/kT}$; hence, the statement on correlation can be reformulated as correlation is obtained if there are terms in the potential energy that cannot be written as a sum of two terms that only depends on either variable. Hence, from eq 1, it is seen that only three terms can contribute to correlation between r_1 and r_2 , namely, the two repulsive terms between the peripheral particles and the polarization term.

A contour plot of the potential in eq 1 is shown in Figure 2. The central particle is charged and either nonpolarizable (upper half) or polarizable (lower half). The parameters in eq 1 are $q = -1e$, $|\mu| = 2.54$ D, $\sigma = \gamma = 1.59$ Å, and $\alpha = 0.0$ or 3.0 Å³. They are set to roughly approximate two water molecules in aqueous solution interacting with a chloride ion in aqueous solution; observe that the construction of the system implies that the individual values of γ and σ are unimportant; only their sum will be of any significance. A symmetric configuration, with the peripheral particles close to the central particle, is the minimum of the potential, both with and without polarizability. The attractive and long-

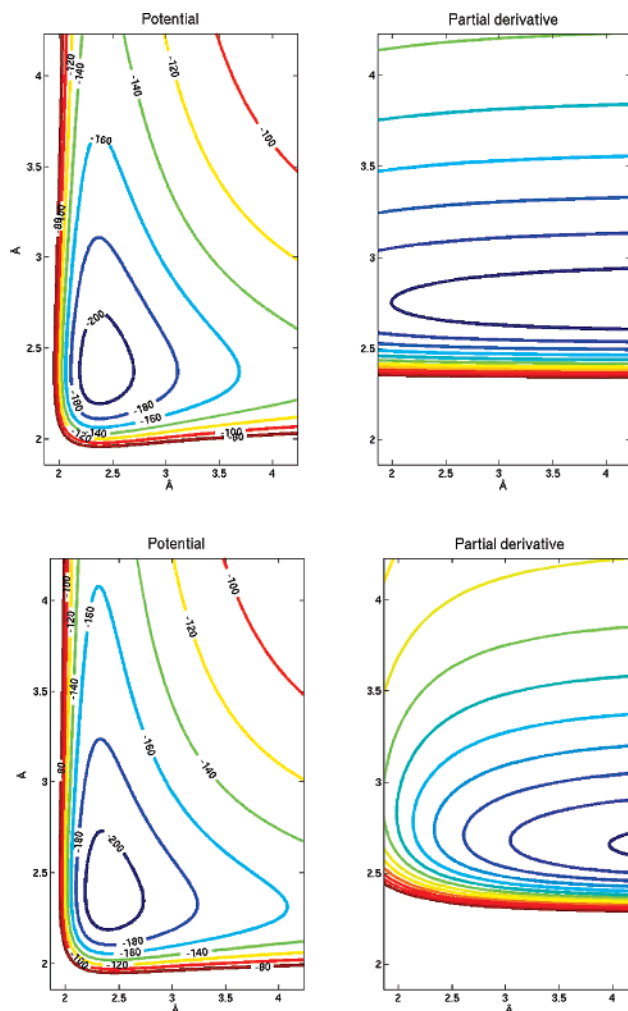


Figure 2. Contour plots of potential (eq 1) for the trimer in kilojoules per mole (left) and the partial derivative along one axis (right). The upper two figures are for a nonpolarizable central particle with charge; the lower ones are for a polarizable central particle with charge.

range charge–dipole pair terms are the reason for this behavior. Only slight differences are seen in the potential plot between the nonpolarizable and polarizable systems. On the right side of Figure 2, the contour plot of the partial derivative $\partial U(r_1, r_2)/\partial r_1$ in an arbitrary unit is shown for the two systems. The contour lines of the nonpolarizable system are almost parallel with the r_2 axis. This implies that the dependence of $U(r_1, r_2)$ on r_1 is almost independent of the value on r_2 (and vice versa from the symmetry of model system A). The slight dependence comes only from the dipole–dipole term, since the polarizability is zero and the Lennard-Jones term between the peripheral particles is at these distances effectively equal to zero. The polarizable system, however, shows a different behavior: the lines are denser at large values of r_2 , and at a decreasing value of r_2 , the contour lines are far from parallel with the axis. The polarization term in the potential thus introduces a much larger coupling between the two degrees of freedom.

To get quantitative information about this coupling, the statistical mechanical problem defined by $U(r_1, r_2)$ is solved at $T = 300$ K. Since the potential is so simple, that problem can be solved essentially exactly by numerical integration.

Table 1. Asymmetry Properties for Ionic Simple Trimer; ρ Is Unitless, $\sqrt{\langle \mathcal{E}^2 \rangle}$ in MV/cm, and Both $\langle |r_1 - r_2| \rangle$ and $\langle r_x \rangle$ in Å; μ in D and α in Å³

μ, q	property	$\alpha = 0.0$	$\alpha = 1.48$	$\alpha = 2.96$	$\alpha = 4.45$	$\alpha = 5.93$
1.02, -1.0	ρ	-0.004	-0.018	-0.033	-0.048	-0.063
	$\sqrt{\langle \mathcal{E}^2 \rangle}$	8.64	8.78	8.92	9.07	9.23
	$\langle r_1 - r_2 \rangle$	0.201	0.205	0.209	0.213	0.217
	$\langle r_x \rangle$	2.679	2.679	2.680	2.681	2.683
		-0.010	-0.061	-0.117	-0.180	-0.249
2.54, -1.0		15.69	16.55	17.56	18.80	20.35
		0.091	0.096	0.102	0.110	0.120
		2.397	2.398	2.399	2.400	2.402
		-0.016	-0.121	-0.249	-0.408	-0.560
		21.87	24.36	27.99	34.09	50.20
4.06, -1.0		0.065	0.073	0.084	0.103	0.154
		2.285	2.286	2.287	2.290	2.301
		-0.002	-0.011	-0.020	-0.024	-0.029
		6.65	6.71	6.77	6.81	6.84
		0.106	0.107	0.108	0.108	0.109
1.02, -2.0		2.449	2.449	2.450	2.450	2.450
		-0.005	-0.037	-0.071	-0.088	-0.107
		12.44	12.85	13.30	13.54	13.80
		0.053	0.055	0.057	0.058	0.059
		2.220	2.221	2.221	2.221	2.221
2.54, -2.0		-0.008	-0.072	-0.144	-0.184	-0.227
		17.33	18.48	19.90	20.75	21.71
		0.038	0.041	0.044	0.046	0.048
		2.118	2.119	2.119	2.119	2.119

Four different quantities are computed: (i) The correlation coefficient

$$\rho(r_1, r_2) = \frac{\langle r_1 r_2 \rangle - \langle r_1 \rangle \langle r_2 \rangle}{\sqrt{(\langle r_1^2 \rangle - \langle r_1 \rangle^2)(\langle r_2^2 \rangle - \langle r_2 \rangle^2)}} \quad (2)$$

where

$$\langle r_x^y \rangle = \frac{1}{\mathcal{Z}} \int \int r_x^y e^{U(r_1, r_2)/kT} dr_2 dr_1$$

and \mathcal{Z} is the partition function is determined. If the degrees of freedom are uncoupled, $\rho(r_1, r_2) = 0$; negative coupling (one large, the other small) leads to a negative correlation coefficient, but not below -1 , and positive coupling leads to positive values, at most 1 . (ii) The square-average electric field on the central particle is also obtained: $\sqrt{\langle \mathcal{E}^2 \rangle}$. It measures how large the electric perturbation from the peripheral particles are, which in a completely symmetric configuration is zero due to cancellation. (iii) The average absolute difference between r_1 and r_2 is computed: $\langle |r_1 - r_2| \rangle$. To interpret this quantity, (iv) the average separations $\langle r_1 \rangle$ and $\langle r_2 \rangle$ are also needed. In Table 1, the quantities i–iv are reported for different dipoles, polarizabilities, and magnitudes of charge. Three noteworthy relations are found: (i) Irrespective of charge or dipole magnitude, an increase in polarizability of the central particle gives rise to an increase of the magnitude of $\rho(r_1, r_2)$, the electric field, $\langle |r_1 - r_2| \rangle$, and $\langle r_x \rangle$. Negative correlation is an effect of asymmetric structures being favored by the increased electric field \mathcal{E} on the polarizable particle in such structures. If only

Table 2. Asymmetry Properties for Quadrupolar Simple Trimer; ρ Is Unitless, $\sqrt{\langle \mathcal{E}^2 \rangle}$ in MV/cm, and Both $\langle |r_1 - r_2| \rangle$ and $\langle r_x \rangle$ in Å; μ in D and α in Å³ and Quadrupole in D·Å

μ, Q_{zz}	property	$\alpha = 0.0$	$\alpha = 4.45$	$\alpha = 8.89$	$\alpha = 14.8$	$\alpha = 26.7$
1.02, -23.8	ρ	-0.004	-0.007	-0.011	-0.016	-0.026
	$\sqrt{\langle \mathcal{E}^2 \rangle}$	2.69	2.70	2.71	2.72	2.74
	$\langle r_1 - r_2 \rangle$	1.845	1.851	1.857	1.865	1.881
	$\langle r_1 \rangle$	6.404	6.404	6.404	6.405	6.405
		-0.006	-0.018	-0.029	-0.045	-0.075
2.54, -23.8		4.92	5.02	5.13	5.29	5.65
		0.418	0.431	0.444	0.464	0.514
		4.586	4.591	4.597	4.605	4.626
		-0.007	-0.027	-0.047	-0.075	-0.128
		5.74	5.87	6.01	6.22	6.76
4.06, -23.8		0.199	0.204	0.209	0.217	0.238
		4.208	4.209	4.210	4.212	4.218
		-0.003	-0.007	-0.010	-0.015	-0.025
		2.72	2.73	2.74	2.75	2.78
		1.192	1.198	1.205	1.213	1.231
1.02, -37.2		5.401	5.404	5.406	5.409	5.415
		-0.003	-0.010	-0.018	-0.028	-0.050
		3.58	3.61	3.64	3.69	3.78
		0.200	0.202	0.203	0.206	0.212
		4.212	4.212	4.213	4.213	4.215
2.54, -37.2		-0.004	-0.017	-0.30	-0.048	-0.087
		4.64	4.70	4.77	4.86	5.06
		0.123	0.124	0.126	0.129	0.134
		3.941	3.941	3.942	3.942	3.943

pair interactions are considered, the dependence of the field could be falsely attributed to stronger interactions from an increased polarizability and hence to a structure with the peripheral particles closer to the central particle. That this is a false argument is seen from $\langle r_x \rangle$ increasing slightly rather than decreasing, so the electric field will not become larger on account of a smaller denominator in the expression for the electric field. (ii) $\sqrt{\langle \mathcal{E}^2 \rangle}$ decreases with an increased charge on the central particle, despite the simultaneous decrease in $\langle r_x \rangle$. The reason is that the importance of the pair terms in the potential increases, and they favor a symmetric configuration, where the electric field is zero. The dependence of the correlation coefficient on the charge confirms this explanation. (iii) With a larger dipole magnitude, the correlation increases for a fixed polarizability, and also, with larger magnitude, the increase of the correlation with polarizability is greater than for the system with a smaller magnitude. This fits well with the prediction that the last term in the potential in eq 1 is the one that mainly determines the degree of correlation.

In Table 2, results from a system with a quadrupole instead of a charge are collected. The Lennard-Jones repulsion is also modified to $\sigma = \gamma = 2.75$ Å, and the quadrupole moment and polarizability are set to qualitatively represent the PBQ–water system. The same relations are found as above, with the only exception being that, for the smallest dipole moment, the electric field increases upon an increased quadrupole moment; this deviation is explained by the correlation being almost unaffected by this modification, while the pair terms see to it that the system gets tighter

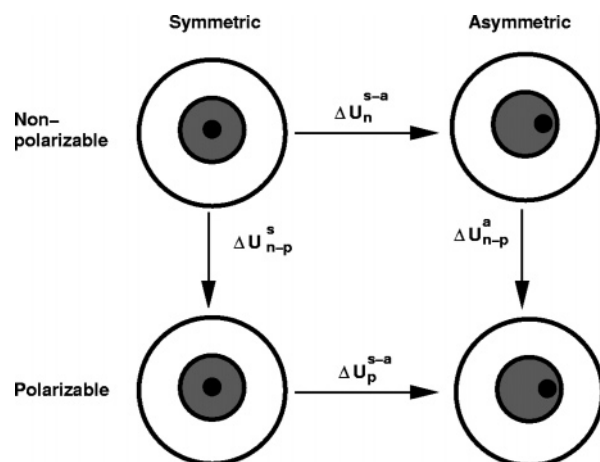


Figure 3. Two-state model system B. All solvent matter included, but separated into two regions: close to the solute particle and far away from the solute particle; the system has two states: symmetric solvation and asymmetric solvation; included in the figure are also the transition energies between the different states.

(see $\langle r_x \rangle$), and that gives a greater field on the central particle. The magnitudes are, however, distinctly different for the quadrupolar system compared to the charged one: the correlation is smaller, and while the increased correlation could lead to a doubling of the field for the charged system, the field is at most increased 20% going from the two extremes in polarizability in Table 2. One reason for this is the weaker pair interactions in the quadrupolar system: With weak interactions, entropy will drive the system to a loose state with the peripheral particles on average far away, which in turn leads to a small field and thus a small correlating energy term in the potential. However, as seen in the charged system with the transition from a monovalent to a divalent system, if entropy is too small, the symmetric energy-minimum configuration will become dominant and that way reduce correlation. Another reason for the small correlation can be that the quadrupolar particle is bigger and the polarization is described with a point polarizability in the middle of the particle, which of course leads to smaller fields; a better description of the polarization of PBQ could change the quantities. To conclude, the two types of model system A have established a few principles and showed that they are the same for charged and quadrupolar systems, while possibly quite different in degree.

2.2. Two-State Many-Body Solvation Model. Model system B is a purely qualitative model for bulk solvation and includes all solvent matter but uses a very simple two-state description of the system, see Figure 3 for illustration. The system is in either a symmetric solvation state or an asymmetric solvation state, and the solvent is divided into two regions, close (gray area in Figure 3) and far away (white area) from the solute (black area). The interaction between the solute and solvent in the former region disrupts what otherwise would be the preferred solvent structure with optimal interactions between the two solvent regions. This implies that, by somehow weakening the solute–solvent interaction, favorable interactions in the entire system can in fact increase (compare this with some explanations of

hydrophobic attraction).^{7–9} Therefore, a transition from the symmetric to asymmetric state, which changes the solute–solvent interaction in the gray region, can be both favorable and unfavorable; which situation that applies is mainly determined by the balance between solute–solvent and solvent–solvent pair interactions. Another feature of model system B is that any transition from the nonpolarizable to polarizable state is favorable. However, it is assumed, on the basis of the results from model system A, that this transition in the asymmetric state is more favorable than that in the symmetric state, that is, $\Delta U_{n-p}^a \leq \Delta U_{n-p}^s \leq 0$. Three cases can be distinguished:

(i) If $\Delta U_n^{s-a} \geq 0$ and $\Delta U_n^{s-a} \geq \Delta U_{n-p}^s - \Delta U_{n-p}^a$, then $\Delta U_p^{s-a} \geq 0$; in other words, in both the nonpolarizable and polarizable states, the symmetric solvation is more probable than the asymmetric solvation.

(ii) If $\Delta U_n^{s-a} \leq 0$, then $\Delta U_p^{s-a} \leq 0$, or in other words, if already the nonpolarizable state favors the asymmetric solvation, the polarizable state will also do so.

(iii) If $\Delta U_n^{s-a} \geq 0$ and $\Delta U_n^{s-a} \leq \Delta U_{n-p}^s - \Delta U_{n-p}^a$, then $\Delta U_p^{s-a} \leq 0$, which means that the introduction of polarizability will turn the system from being preferably symmetrically to asymmetrically solvated.

Model system B shows that, with the entire solvent (or a sufficient amount, at least) in the treatment, other factors related to the balance between the different interactions in the system become important in understanding the structure around the solute and hence the solvent effects. The qualitative nature of the model and its unrealistic account of entropy precludes any predictions for specific systems, however. Hence, model system B is only a thought experiment to warn against interpretations based only on the solvent in contact with the solute, as in the preceding model system A.

2.3. Explicit Many-Body Solvation. An accurate description of a solvation phenomenon requires that both features of model systems A and B be taken into account, that is, a plausible description of the interactions and the thermodynamics of the system, and that a sufficient portion of the solvent–solvent interactions be accounted for to adequately describe their indirect effect on the solute–solvent interaction. An obstacle, on the conceptual level, is that, once both features are combined, it is not as easy to analyze the system as in model systems A and B, and this results in observations that are not easy to trace. This also makes predictions based only on simple physical relations of the constituents more difficult to make. It may, however, be that the simultaneous introduction of both features invalidates questions about causation of a nature as precise as that in the previous two models. A system in its full complexity may very well entangle the causes and therefore, on a fundamental level, rule out clear statements on cause and effect in the present state of the theoretical development. Before this discussion is continued in a section below, a simulation of a solute–solvent system in its full complexity is done, both with a polarizable and a nonpolarizable solute. This provides one particular realistic system from which limited generalization can be made.

The easiest system would be a monatomic ion in a polar solvent. These systems have already been extensively studied

with Monte Carlo and molecular dynamics simulations, and their results will be discussed from the present perspective below.^{2–6,10–16} As noted in the Introduction, it has recently been established that similar questions on solvent structure and correlation are meaningful also for neutral solutes.¹ The neutral and non-dipolar PBQ in aqueous solution is chosen as the model system.

The model used is the combined quantum chemical statistical mechanical solvent model called QMSTAT.¹⁷ In the present simulation, a Hartree–Fock (HF) wave function is used for PBQ since only the electronic ground state of PBQ is relevant; an extension of QMSTAT for excited states has been formulated and was used in the previous study on PBQ and its electronic spectrum.^{1,18} The model solves the quantum chemical problem in a truncated natural molecular orbital basis. The model is thus compact, and the small dimension of the Fock matrix as well as the ability to store all two-electron integrals in memory leads to a single calculation being a relatively easy task. In the subsequent Monte Carlo simulation, it is then tenable to solve a quantum chemical problem in each step. Therefore, the combined quantum chemical statistical mechanical problem can be solved with a so-called hybrid approach which enables the statistical error to be made arbitrarily small, as compared to the more common but approximate sequential approach. Since a key aspect in the present study is the polarization of the solute and its consequences on statistical solvent properties, QMSTAT is a suitable model since both polarization and statistical mechanics are treated well. Details of QMSTAT are available elsewhere, and below only the particular aspects for PBQ are presented.^{17,18} The Møller–Plesset optimized structure is used for PBQ (same as in ref 1).¹⁹ An atomic natural orbital (ANO) basis set is used for all orbital calculations; contractions are C,O 4s3p2d; H 2s1p.²⁰ The natural orbitals are constructed from diagonalization of an average density matrix; the different density matrices adding up to the average comes from HF calculations with the same set of perturbations as in the inhomogeneous basis in ref 1. For the nonpolarizable system, only occupied orbitals are included in the basis; hence, the electronic wave function has no flexibility and is frozen in its gas-phase form. For the polarizable state, 42 orbitals are included in total, which retains almost all polarizability that the full ANO-basis set gives. Solute–solvent dispersion interaction is parametrized as in ref 1, and the repulsive solute–solvent pseudo-potential parameters are $d = -0.32$ and $\beta_4 = 2.5$ (see ref 18 for relevant equations). A total of 150 explicit polarizable water molecules are included as the solvent, and a nonperiodic boundary condition using the image-charge approximation is added.^{21–23} To rule out statistical uncertainties for the observed properties, special attention is paid to the convergence of the Monte Carlo simulation and the statistical significance of computed quantities; this technical discussion is put in Appendix A. Statistical properties are computed from simulations of 4.2×10^6 Monte Carlo steps where every 100th configuration is sampled. All quantum chemical calculations are done with the quantum chemical software package MOLCAS, which also is the platform for the development of QMSTAT.^{24,25}

Table 3. Quantities and 99.9% Confidence Intervals from Simulation on PBQ, with and without Polarization^a

	no polarization		with polarization	
	average	conf. int.	average	conf. int.
$\rho(r_1, r_2)$	−0.032	(−0.047, −0.016)	−0.166	(−0.181, −0.151)
$\langle r_1 - r_2 \rangle$	0.316	(0.312, 0.319)	0.313	(0.309, 0.317)
$\rho(\phi(r_1), \phi(r_2))$	0.043	(0.027, 0.060)	−0.114	(−0.130, −0.097)
$^{1/2}\langle \phi(r_1) + \phi(r_2) \rangle$	0.380	(0.375, 0.384)	0.512	(0.507, 0.516)
$\sigma(^{1/2}\langle \phi(r_1) + \phi(r_2) \rangle)$	0.284	(0.270, 0.297)	0.296	(0.278, 0.312)

^a Distances in Å and potentials in V.

In this complex system, an analysis of asymmetry and correlation in the solvent structure is more difficult. No clear-cut choice of quantities to characterize the degree of asymmetry is evident to us. To achieve a close correspondence between the results of this model and the results of model system A, however, five different quantities are chosen. (i) The correlation coefficient (eq 2) for r_1 and r_2 is computed, where r_1 and r_2 are defined as the shortest distance between a hydrogen atom in the solvent and the oppositely located oxygen atoms of PBQ. This corresponds to $\rho(r_1, r_2)$ in model system A. (ii) The average difference $\langle |r_1 - r_2| \rangle$, which corresponds to the same type of quantity in model system A, is obtained. (iii) Next, the correlation coefficient between $\phi(x_1)$ and $\phi(x_2)$, where $\phi(x_1)$ is the electric potential from the solvent at one of the oxygen atoms in PBQ, is determined; $\phi(x_2)$ is the corresponding quantity at the other oxygen atom. This corresponds in part to $\sqrt{\langle \mathcal{E}^2 \rangle}$ in model system A, since it measures the correlation of the electric perturbation on the solute. The magnitude of the electric field in the middle of PBQ, which superficially has more in common with $\sqrt{\langle \mathcal{E}^2 \rangle}$, is a less adequate measure since it implicitly assumes that a polarizability in the center of mass best characterizes the polarization of PBQ in aqueous solution, which hardly is a valid approximation to the polarization in QMSTAT. (iv) Finally, the average value of $\phi(x_1)$ and $\phi(x_2)$ and (v) their standard deviation are evaluated. Although they do not measure the degree of asymmetry or correlation, they show what effect the polarization will have on the magnitude of the electric perturbation from the solvent on the solute, which in part also corresponds to $\sqrt{\langle \mathcal{E}^2 \rangle}$ in model system A. The quantities are reported in Table 3 with 99.9% confidence intervals obtained with the bootstrap method (see Appendix A).

In Table 3, it is seen that both correlation coefficients i and iii are significantly different between nonpolarizable and polarizable PBQ. For the nonpolarizable PBQ, a faint correlation is found, while polarizable PBQ has a negative correlation between both r_1 and r_2 , as well as $\phi(x_1)$ and $\phi(x_2)$. The average of $|r_1 - r_2|$ is not significantly different between the two system, however. The reason for this is that two effects cancel: on the one hand, the more negative correlation in the polarizable state increases the difference; on the other hand, the shorter separation between the solute and solvent in the same state decreases the difference; see Figure 4 for the radial distribution functions which prove the latter statement. Further, the solvent electric potential on the oxygen atoms is significantly larger in the polarizable state. The standard deviation, however, has no significant

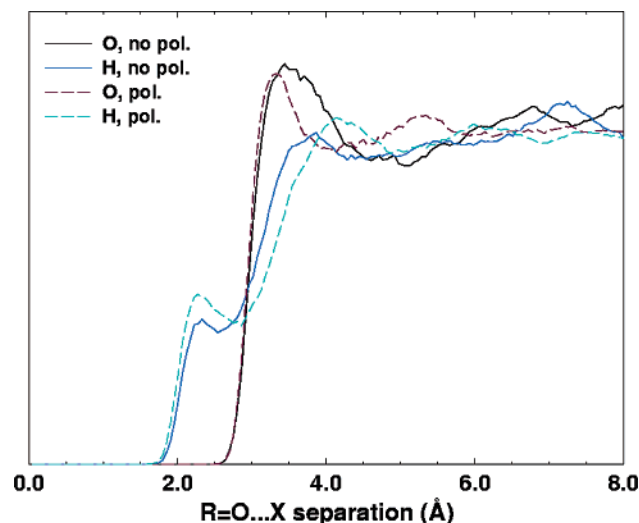


Figure 4. Radial distribution functions around the oxygen atoms for nonpolarizable and polarizable PBQ in an aqueous solution.

difference between the two systems. The reason the average is larger will to some extent be explained by the increased asymmetry in the polarizable state. That is probably not the entire reason, though. An additional contribution is likely to come from the increased reaction field from the polarizable solvent when the solute polarizes.

3. Discussion

Asymmetric solvent configurations are themselves nothing novel: thermal fluctuations, or entropy, will always, at nonzero temperatures, lead to configurations outside of the, possibly, symmetric energy minimum; see, for example, $\sqrt{\langle \mathcal{E}^2 \rangle}$ in Tables 1 and 2 at zero polarizability where the nonzero value comes only from the aforementioned fluctuations and not from the correlation discussed above. Still, the average over all configurations may be symmetric. This observation leads to a critique of the mean-field approximation, which is the basis for the widespread continuum solvent models. There, the solute interacts with the field from the average solvent configuration, which as observed above may be a symmetric one with zero electric field. If the particle solvated in the dielectric cavity is polarizable, an attractive term will be missing because fluctuations are missing. This critique has been formalized elsewhere, and corrections to continuum solvent models have been proposed.^{26–28} Other problems with the continuum models are discussed by de Vries et al.²⁹

Model system A, above, shows that the thermal molecular fluctuations can be correlated. The polarizability will not only interact favorably with the fluctuation field coming from independent random fluctuations (i.e., the electric field at $\alpha = 0$ in model system A) but will couple the solvent degrees of freedom and enhance the magnitude of the fluctuating electric field on the solute. To put it differently, model system A shows that polarization can introduce a bias for asymmetric solvent configurations and, by that, increase the magnitude of the fluctuations.

Results from simulations of monatomic and lately also polyatomic ions in aqueous solution have in some cases been

interpreted in similar terms. Bulk simulations by Carignano et al. of ions with variable polarizability, but with fixed sizes, have shown that the solvation environment tends to get more asymmetric with increasing polarizability for a fixed size.¹⁰ Other simulations of highly polarizable anions in bulk show that the structure in the closest hydration shell is less symmetric than in less polarizable ions, although other effects are not always ruled out.^{11–13} Wilson and Madden have also argued that layered structures for certain simple ionic compounds are effects of anion polarizability and their affinity for asymmetric environments.^{30,31} Results from simulations on the distribution of ions between bulk and air/water interfaces have also been shown to be dependent on the polarizability of the ionic solute.^{2–6} The air/water interface can be seen as an extreme asymmetric environment. Thus, the polarizability of the ion, in the same fashion as in model system A, increases the probability for the interface to be populated as compared to the less asymmetric bulk environment. But clearly, other factors will have an influence, as the simple thought experiment in model system B shows. Hrobárik et al. give a lucid example with several tetraalkylammonium cations with different alkyl chain lengths: the different surface propensities of the ions are rationalized by the increasing hydrophobicity of the ion with increasing chain length.⁶ And there are studies on monatomic ions that establish and emphasize the importance of the balance between solute–solvent and solvent–solvent interactions also for these systems.^{4,11,14–16,32} A recent experiment also found that surface affinity correlates most strongly with ion size, not polarizability.³³ As a final remark, however, we observe that the polarizability of molecules in solution, and anions in particular, is a property that depends on the environment and is consequently not easy to unequivocally assign.^{34–39}

PBQ is neutral but has a significant quadrupole moment due to the polar carbonyl groups. Interactions with quadrupoles can be large, and to consider them insignificant is in many applications quite wrong.^{40–43} Also, as shown with model system A, the same principles that apply to the ionic system with respect to correlation of the solvent degrees of freedom by polarization apply also to the quadrupolar system. Further, we established above in a detailed simulation that there is a significant difference in the correlation with and without polarizability on PBQ. Together, these two results strongly suggest that it is the polarization of PBQ that couples the solvent degrees of freedom on opposite sides of the solute molecule by the same simple mechanism that operates in model system A. As shown with that model system, however, a polarizability is not enough to cause correlation; there has to be favorable solute–solvent pair terms that order the solvent adjacent to the solute for a significant fluctuation field to appear on the solute. In the most weakly interacting case for model system A, entropy almost manages to dissociate the solute–solvent system. In the simulation of PBQ, packing effects will, however, make the space close to PBQ occupied at all times; instead, other degrees of freedom can be used to contain the hydrophobic solute so that the solvent–solvent interactions are minimally perturbed. Dominance of such configurations implies a small fluctuation

field on the solute. Therefore, the hydrogen bonds between water and the carbonyl oxygen atom (primarily a pair term) have an indirect but important effect on the correlation.

It is important to observe, though, that the hypothesis only deals with why the correlation exists and its implications on the fluctuation field. The details from which the actual magnitude of the fluctuation field could be computed are not dealt with. In model system A, it is shown that the correlation and the electric field on the solute have the same type of dependence on the polarizability no matter what charge or quadrupole the central particle has. But the magnitude of the field depends on these central particle properties for reasons discussed above. For a complex system such as PBQ in aqueous solution, several specific features of the system will contribute to this, and we do not propose to have a quantitative theory for this intricate problem.

Solvent effects on chemical reactions, absorption and fluorescence spectra, and many other relevant processes are effects of the electric perturbation the solvent exerts on the solute.⁴⁴ From the perspective of a mean-field theory of the solvent, this perturbation will be small for molecules with no dipole and be of the same symmetry as the solute molecule. As previously discussed, this will lead to the neglect of a stabilizing fluctuation term. Another effect is that symmetry-breaking terms that should appear in the Hamiltonian are lost. For example, in the study of nonlinear optics, quadrupolar (or higher) chromophores are often used, and their electronic ground and, more often, excited states can be quite labile to symmetry-breaking terms in the Hamiltonian and through them give rise to distinct modifications compared to gas-phase or other nonpolar surroundings.^{45–47} The excited state from the one-photon excitation $n \rightarrow \pi^*$ in PBQ is in fact near-degenerate, and therefore the solvated state undergoes a large mixing because there is a significant symmetry-broken term in the effective Hamiltonian from the solvent.¹ Zijlstra et al. also show how drastic the effects of solvent-induced symmetry breaking are on excited ethylene.⁴⁸ As shown here, the magnitude of this symmetry-breaking perturbation in these and similar systems can be even larger than expected since correlations caused by the polarizability and the discrete molecular nature of the solvent are likely to exist.

4. Conclusions

Starting from a very simple model of a non-dipolar molecule in a polar surrounding, and going to a simulation of great detail, we have found support for the hypothesis that the many-body nature of the polarization of the non-dipolar solute couples the solvent degrees of freedom in such a way that asymmetric solvent configurations are favored. In asymmetric configurations, the electric perturbation from the solvent on the solute is larger, which leads to an increase in magnitude of the fluctuating field, implied by the thermal fluctuations of the solvent, with an increase of the polarizability of the solute. However, the pair interactions between the solute and solvent must also be included in the explanation since they have an indirect effect on the correlation and the fluctuations. The mechanism we propose is valid for the solvation of both ions and quadrupolar molecules, and we

comment on previous studies of ion solvation and the surface affinity of ions. Other situations where this can be of relevance is in understanding solvent effects on multipolar molecules. The present study highlights the intricacy of the fluctuating electric field a molecule experiences in a solvent.

Acknowledgment. Financial support from the Swedish Research Council within the Linné-project Organizing Molecular Matter is acknowledged. Computer time at Lunarc, Center for Scientific and Technical Computing, Lund University is acknowledged.

Appendix A

To obtain statistically certain quantities for the QMSTAT simulation of PBQ in water, convergence diagnostics and bootstrap confidence intervals are used. Both methods are described below.

In any Monte Carlo simulation of a complex system, knowing when a balanced sampling of the configuration space has been achieved is difficult. This problem is especially critical when free-energy barriers exist in the system. Brooks and Gelman have proposed a simple convergence diagnostic, which has become popular in applications of Monte Carlo statistical techniques in medicine.⁴⁹ Other more advanced diagnostics exist, but the Brook–Gelman diagnostic (BGD) is judged to be of sufficient accuracy for the present application and also has a feature that fits well with our simulation approach.⁵⁰

To obtain the BGD, (i) N parallel Monte Carlo simulations with different initial configurations are run for m steps each. (ii) Some measure (vide infra) of variance is computed between the different chains of configurations as well as within the chains. If these measures differ significantly, that tells that the individual chains have not been sampled over a sufficient space, and m should be increased. (iii) When between and within measures are of similar value, convergence is likely to have been reached, although it does not guarantee convergence

Two different measures of variance are used, both proposed by Brooks and Gelman (observe that a different notation is used in ref 49). First, the second moments:

$$\hat{B}_2 = \frac{1}{Nm - 1} \sum_{i,j}^{N,m} (x_{ij} - x_{..})^2$$

$$\hat{W}_2 = \frac{1}{N(m - 1)} \sum_{i,j}^{N,m} (x_{ij} - x_{i.})^2$$

where x_{ij} is the j th element in the i th chain, and a dot in the indices means that that index has been averaged. Another measure is

$$\hat{L}_B = |l_i^{\text{tot}} - l_r^{\text{tot}}|$$

$$\hat{L}_W = \frac{1}{N} \sum_i^N |l_i^i - l_r^i|$$

where l_i^i and l_r^i are the estimated confidence interval limits for $\{x_{ij}\}_{j=1,\dots,m}$ for a given chain i , and l_i^{tot} and l_r^{tot} are the

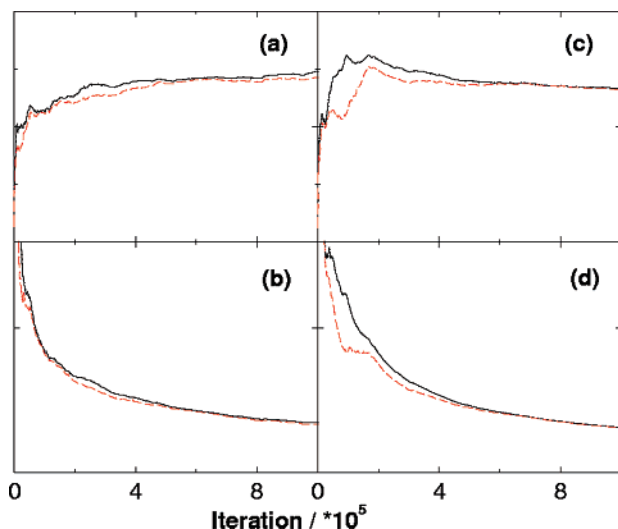


Figure 5. (a) The second moment of the minimum oxygen–hydrogen atom distance on one side of nonpolarizable PBQ. Part c is like a, only that PBQ is polarizable. Diagrams b and d show the confidence interval width for nonpolarizable and polarizable PBQ, respectively. All black lines are the between measure; all red dashed lines are the within measures.

same for the entire data set. Observe that $\hat{L}_B \sim 1/\sqrt{m}$ as $m \rightarrow \infty$; the same goes for \hat{L}_W . In Figure 5, the progression of the measures as longer individual Monte Carlo chains are sampled is shown; four parallel chains have been used. The sampled quantities x_{ij} are the shortest distance between a specific oxygen atom on PBQ and the hydrogen atoms of the solvent. As can be seen, the measures have converged to being very close to each other in both cases. Other quantities x_{ij} of the simulation show the same behavior. This suggests (but does not prove) that convergence has been reached and that the total data set is a balanced sample of the relevant configuration space. Observe that the equilibration period (called burn-in period in ref 49) is not included in Figure 5.

The bootstrap method is a resampling method constructed by Efron.⁵¹ It is a method that can be used to solve statistical problems of a very diverse nature, even when the knowledge of the probability distribution is incomplete. For the present study, it is used to construct confidence intervals in Table 3, an application for which bootstrap is suitable.⁵² A premise for this method is that the samples are collected from independent distributions. In a Monte Carlo simulation, this is not fulfilled. However, the bootstrap method can still be used if the collected sample is a balanced sample of the configuration space, or in other words, where the set of sampled points appears as if they were obtained independently. Therefore, to apply the bootstrap method properly, convergence has to be reached in the sense described above in relation with BGD. Once this is established, the nonparametric percentile bootstrap method is applied to construct confidence intervals for the correlation coefficients and the other variables. A description of this method can be found in advanced textbooks on statistical inference or on resampling methods.

References

- (1) Öhrn, A.; Aquilante, F. *Phys. Chem. Chem. Phys.* **2007**, *9*, 470–480.
- (2) Jungwirth, P.; Tobias, D. J. *J. Phys. Chem. B* **2002**, *106*, 6361–6373.
- (3) Karlström, G.; Hagberg, D. *J. Phys. Chem. B* **2002**, *106*, 11585–11592.
- (4) Hagberg, D.; Brdarski, S.; Karlström, G. *J. Phys. Chem. B* **2005**, *109*, 4111–4117.
- (5) Jungwirth, P.; Tobias, D. J. *Chem. Rev.* **2006**, *106*, 1259–1281.
- (6) Hrobárik, T.; Vrbka, L.; Jungwirth, P. *Biophys. Chem.* **2006**, *124*, 238–242.
- (7) Israelachvili, J. N. *Intermolecular and Surface Forces*, 2nd ed.; Academic Press: London, Great Britain, 1992.
- (8) Forsman, J.; Jönsson, B.; Woodward, C. E. *J. Phys. Chem.* **1996**, *100*, 15005–15010.
- (9) Meyer, E. E.; Rosenberg, K. J.; Israelachvili, J. *Proc. Natl. Acad. Sci. U.S.A.* **2006**, *103*, 15739–15746.
- (10) Carignano, M. A.; Karlström, G.; Linse, P. *J. Phys. Chem. B* **1997**, *101*, 1142–1147.
- (11) Raugei, S.; Klein, M. L. *J. Chem. Phys.* **2002**, *116*, 196–202.
- (12) Rajamani, S.; Ghosh, T.; Garde, S. *J. Chem. Phys.* **2004**, *120*, 4457–4466.
- (13) Tofteberg, T.; Öhrn, A.; Karlström, G. *Chem. Phys. Lett.* **2006**, *429*, 436–439.
- (14) Perera, L.; Berkowitz, M. L. *J. Chem. Phys.* **1992**, *96*, 8288–8294.
- (15) Stuart, S. J.; Berne, B. J. *J. Phys. Chem.* **1996**, *100*, 11934–11943.
- (16) Grossfield, A. *J. Chem. Phys.* **2005**, *122*, 024506.
- (17) Moriarty, N. W.; Karlström, G. *J. Phys. Chem.* **1996**, *100*, 17791–17796.
- (18) Öhrn, A.; Karlström, G. *Mol. Phys.* **2006**, *104*, 3087–3099.
- (19) Møller, C.; Plesset, M. S. *Phys. Rev.* **1934**, *46*, 618–622.
- (20) Pierloot, K.; Dumez, B.; Widmark, P.-O.; Roos, B. O. *Theor. Chim. Acta* **1995**, *90*, 87–114.
- (21) Wallqvist, A.; Ahlström, P.; Karlström, G. *J. Phys. Chem.* **1990**, *94*, 1649–1656.
- (22) Friedman, H. L. *Mol. Phys.* **1975**, *29*, 1533–1539.
- (23) Wallqvist, A. *Mol. Simul.* **1993**, *10*, 13–17.
- (24) Karlström, G.; Lindh, R.; Malmqvist, P.-Å.; Roos, B. O.; Ryde, U.; Veryazov, V.; Widmark, P.-O.; Cossi, M.; Schimelpennig, B.; Neogrady, P.; Seijo, L. *Comput. Mater. Sci.* **2003**, *28*, 222–239.
- (25) Veryazov, V.; Widmark, P.-O.; Serrano-Andrés, L.; Lindh, R.; Roos, B. O. *Int. J. Quantum Chem.* **2004**, *100*, 626–635.
- (26) Baur, M. E.; Nicol, M. *J. Chem. Phys.* **1966**, *44*, 3337–3343.
- (27) Karlström, G.; Halle, B. *J. Chem. Phys.* **1993**, *99*, 8056–8062.

- (28) Sánchez, M. L.; Martín, M. E.; Galván, I. F.; Olivares del Valle, F. J.; Aguilar, M. A. *J. Phys. Chem. B* **2002**, *106*, 4813–4817.
- (29) de Vries, A. H.; van Duijnen, P. T.; Juffer, A. H. *Int. J. Quantum Chem., Quantum Chem. Symp.* **1993**, *27*, 451–466.
- (30) Wilson, M.; Madden, P. A. *J. Phys.: Condens. Matter* **1994**, *6*, 159–170.
- (31) Stone, A. J. *The Theory of Intermolecular Forces*, 1st ed.; Oxford University Press: Oxford, Great Britain, 1996.
- (32) Frank, H. S.; Wen, W.-Y. *Discuss. Faraday Soc.* **1957**, *24*, 133–140.
- (33) Cheng, J.; Vecitis, C. D.; Hoffmann, M. R.; Colussi, A. J. *J. Phys. Chem. B* **2006**, *110*, 25598–25602.
- (34) Mayer, J. E.; Mayer, M. G. *Phys. Rev.* **1933**, *43*, 605–611.
- (35) Pyper, N. C.; Pike, C. G.; Edwards, P. P. *Mol. Phys.* **1992**, *76*, 353–372.
- (36) Giese, T. J.; York, D. M. *J. Chem. Phys.* **2004**, *120*, 9903–9906.
- (37) Öhrn, A.; Karlström, G. *J. Phys. Chem. B* **2004**, *108*, 8452–8459.
- (38) Krishtal, A.; Senet, P.; Yang, M.; van Alsenoy, C. *J. Chem. Phys.* **2006**, *125*, 034312.
- (39) Heaton, R. J.; Madden, P. A.; Clark, S. J.; Jahn, S. *J. Chem. Phys.* **2006**, *125*, 144104.
- (40) Buckingham, A. D.; Fowler, P. W. *J. Chem. Phys.* **1983**, *79*, 6426–6428.
- (41) Hurst, G. J. B.; Fowler, P. W.; Stone, A. J.; Buckingham, A. D. *Int. J. Quantum Chem.* **1986**, *29*, 1223–1239.
- (42) Moriarty, N. W.; Karlström, G. *J. Chem. Phys.* **1997**, *106*, 6470–6474.
- (43) Zhao, X. C.; Johnson, J. K. *Mol. Simul.* **2005**, *31*, 1–10.
- (44) Reichardt, C. *Solvents and Solvent Effects in Organic Chemistry*, 3rd ed.; Wiley-VCH: Weinheim, Germany, 2003.
- (45) Droumaguet, C. L.; Mongin, O.; Werts, M. H. V.; Blanchard-Desce, M. *Chem. Commun.* **2005**, 2802–2804.
- (46) Terenziani, F.; Painelli, A.; Katan, C.; Charlot, M.; Blanchard-Desce, M. *J. Am. Chem. Soc.* **2006**, *128*, 15742–15755.
- (47) Bidault, S.; Brasselet, S.; Zyss, J.; Maury, O.; Bozec, H. L. *J. Chem. Phys.* **2007**, *126*, 034312.
- (48) Zijlstra, R. W. J.; Grozema, F. C.; Swart, M.; Feringa, B. L.; van Duijnen, P. T. *J. Phys. Chem. A* **2001**, *105*, 3583–3590.
- (49) Brooks, S. P.; Gelman, A. *J. Comput. Graph. Stat.* **1998**, *7*, 434–455.
- (50) Brooks, S. P.; Roberts, G. O. *Stat. Comput.* **1998**, *8*, 319–335.
- (51) Efron, B. *Ann. Stat.* **1979**, *7*, 1–26.
- (52) Efron, B.; Tibshirani, R. *Stat. Sci.* **1986**, *1*, 54–75.

CT700022B